Histol Histopathol (2025) 40: 1415-1423

Histology and Histopathology
From Cell Biology to Tissue Engineering

ORIGINAL ARTICLE Open Access

Rosmarinic acid inhibits the proliferation of ovarian carcinoma cells by activating the p53/BAX signaling pathway

İlhan Özdemır[1], Dilek Doğan Baş[2], Şamil Öztürk[3], Özge Karaosmanoğlu[4] and Mehmet Cudi Tuncer[5]

[1]Department of Gynecology and Obstetrics, Faculty of Medicine, Atatürk University, Erzurum, [2]Women's Health and Obstetrics Clinic, Bursa, [3]Vocational School of Health Care Services, Çanakkale Onsekiz Mart University, Çanakkale, [4]Acibadem Maslak Hospital IVF Clinic, İstanbul and [5]Dicle University, Faculty of Medicine, Department of Anatomy, Diyarbakir, Turkey

Summary. Objective. While chemotherapeutic agents stop the development of cancer cells, they also kill healthy cells. This study aimed to increase anticancer effects and reduce side effects by combining a phytotherapeutic compound with a chemotherapeutic drug.

Methods. This study examined the effects of nine concentrations of rosmarinic acid (RA) and doxorubicin (DOX) on human ovarian adenocarcinoma (OVCAR3) and skin keratinocyte (HaCaT) cell lines. Their cytotoxic effects were assessed based on cell viability, evaluated using the MTT assay, and apoptotic activity, evaluated using NucBlue staining and the gene and protein expression of tumor protein p53 (TP53) and BCL2 associated X, apoptosis regulator (BAX) quantified by qRT-PCR and western blots, respectively.

Results. The half-maximal inhibitory concentration after 48 hours was 880.4 μM for RA and 2.26 μM for DOX. The cytotoxicity analysis revealed that cell viability decreased with the RA concentration. RA increased apoptosis in OVCAR3 cells by activating the p53/BAX pathway. Western blots showed that RA and DOX upregulated p53 and BAX protein levels in OVCAR3 cells.

Conclusions. The RA and DOX combination inhibited cell proliferation by inducing apoptosis in OVCAR3 cells. These results suggest that RA may reduce the side effects of DOX toxicity.

Key words: Rosmarinic acid, Ovarian cancer, OVCAR3, Apoptosis, qRT-PCR, Cell death

Corresponding Author: M. Cudi Tuncer, Professor, Ph.D., Dicle University, Medical School, Chief of Anatomy Department, Diyarbakır, Turkey. e-mail: drcudi@hotmail.com

www.hh.um.es. DOI: 10.14670/HH-18-883

Introduction

Rosmarinic acid (RA) is a flavonoid widely found in plants belonging to the Lamiaceae family. Plants known to be rich in RA, especially *Perilla frutescens* (L.) Britton, *Rosmarinus officinalis* L., and *Melissa officinalis* L., remain popular worldwide and are used in tea, herbs, food condiments, spices, and fruits. However, studies have shown that RA has strong antioxidant activity and the potential to treat cancer due to its nutritional properties (Magalhães et al., 2018). Recent studies have revealed that these plants can prevent and treat cancer. In addition, studies isolating the antitumor components of the plant have shown that their active components include polyphenols and positively affect the treatment process. Moreover, these studies have revealed that RA can stop tumor development and growth and sensitize them to chemo-radiotherapy agents (Jin et al., 2021). How RA is prepared is crucial. Studies suggest that RA should be synthesized by engineering bacteria *in vitro*, especially due to its dependence on purification after biosynthesis in plants. Since RA has low bioavailability, the dosage form must be improved, and chemical delivery systems must be developed if it is to be used for antitumor treatments (Achour et al., 2021).

Cancer is an important public health issue that continues to increase worldwide. Cancer treatments have advanced significantly in recent years with the development of new technologies, including the application of surgical procedures in cancer treatments, especially treatment methods and immunotherapies targeting cancer cells. Therefore, newly developed treatments have significantly advanced the fight against cancer. However, while preliminary interventions are being evaluated and new treatment methods are being developed to treat cancer, tumor progression and post-treatment drug resistance remain the most critical aspects of clinical oncology (Siegel et al., 2022).

As serious challenges in the fight against cancer,

lengthy treatments and repeated hospitalizations significantly affect patients' quality of life and cause them severe psychological stress (Emery et al., 2022). Studies have used dietary supplements and some herbal products in cancer treatment to prevent tumor development, demonstrating their effects during treatment (Ganesan et al., 2022). Ovarian cancer is known to be the deadliest gynecological cancer globally. Studies have shown that it constitutes 2.5% of all malignancies, especially in women (Torre et al., 2018). The primary treatment goal in ovarian cancer is to destroy the remaining cancer cells through surgery and chemotherapy. During cancer treatment, many patients become resistant to chemotherapy drugs, especially cisplatin (Pokhriyal et al., 2019). For this reason, many researchers are conducting many studies and looking for new models to eliminate the side effects of chemotherapy applied for the treatment of ovarian cancer (Chandra et al., 2019). In recent years, studies have sought to eliminate drug resistance in cancer cells, especially using herbal products (Homayoun et al., 2015).

Ovarian carcinoma is one of the most lethal gynecological malignancies, characterized by late-stage diagnosis and a high rate of chemoresistance. The search for novel therapeutic agents that effectively target ovarian cancer cells with minimal side effects is ongoing. RA, a naturally occurring polyphenolic compound found in various plants, has been reported to possess anti-inflammatory, antioxidant, and anticancer properties. However, the mechanisms underlying its anticancer effects, particularly in ovarian carcinoma, remain to be fully elucidated. Therefore, in this study, we aimed to investigate the potential of RA to inhibit the proliferation of ovarian carcinoma cells and decipher the molecular pathways involved. We focused on the tumor protein p53 (TP53)/BCL2 associated X, apoptosis regulator (BAX) signaling pathway, a crucial mediator of cell cycle regulation and apoptosis. By examining the effects of RA on this pathway, we aimed to provide insights into its therapeutic potential and the mechanistic basis of its anticancer activity.

Materials and methods

Cell culture

This study used OVCAR3 (American Type Culture Collection [ATCC]: HTB-161) and HaCaT (RRID: CVCL_0038) obtained from the ATCC. The cells arrived frozen in a cryotube and were kept in a hot water bath at 37°C for 1-2 minutes before being removed, completely dissolved, and transferred to a 15 mL falcon containing 3 mL of medium. Next, the tube was centrifuged at 800 rpm for 5 minutes, the supernatant was discarded, and 1 mL of medium was added to the cells and gently pipetted. Then, the suspended cells were transferred to a 75 cm^2 flask containing RPMI 1640 medium, 10% fetal bovine serum, 2 mM L-glutamine, and 1% penicillin/streptomycin. The flasks were placed in an incubator at 37°C with 5% CO_2 for healthy cell confluency.

Mycoplasma contamination

Mycoplasma contamination of the studied cell lines was assessed by DNA fluorescence labeling with bisbenzimide (Hoechst 33258, Sigma-Aldrich).

Cell viability

From a suspension with a determined number of cells, 5×10^3 cells were seeded in each well of a 96-well plate. Then, the plate was incubated at 37°C with 5% CO_2. Nine different doses of RA (10-1000 µM) and doxorubicin (DOX; 0.5-50 µM) were applied; the same volume of medium was added to the control group. After drug addition, the plate was incubated for 24, 48, or 72 hours. After incubation, 30 µL of 3-(4,5-dimethylthiazol-2-yl)-2,5-diphenyltetrazolium bromide (MTT) solution was added to each well and incubated for 3 hours. Next, the medium was removed from the wells using a pipette, and 200 µL of dimethyl sulfoxide, which dissolves formazan crystals, was added. After 15 minutes, the dissolved formazans were measured by absorbance at 492-650 nm with a GO microplate reader.

Cytotoxicity

The OVCAR3 and HaCat cells were treated with nine different concentrations of RA (10-1000 µM) and DOX (0.5-50 µM). The half-maximal inhibitory concentrations (IC_{50}) of the vehicle and trial groups were calculated using the statistical program based on the effects of the different RA and DOX concentrations on cell viability in the MTT assay. Once the IC_{50} was determined, that dose was applied to analyze more specific results.

Nuclear staining assay

The NucBlue® Live ReadyProbes® Reagent (Thermo Fisher Scientific, USA) was used to determine nuclear morphology changes and apoptotic structures after apoptosis in OVCAR3 cells caused by DOX and RA.

Total RNA isolation and cDNA synthesis

OVCAR3 cells were seeded in 25 cm^2 culture flasks and incubated until they reached the logarithmic phase. Next, they were treated with the vehicle (control), DOX (IC_{50}), RA (IC_{50}), or DOX+RA (IC50) for 72 hours. Then, their total RNA was isolated using the Purelink RNA Mini Kit (Thermo Fisher Scientific, USA) according to the manufacturer's instructions. The purity of the isolated RNA was determined using the Optizen NanoQ microvolume spectrophotometer (Mecasys,

South Korea). Then, each RNA sample was diluted with ultrapure water to 750 ng/10 µL. Next, complementary DNA (cDNA) was synthesized. Then, the cDNAs were amplified using the quantitative reverse transcription-polymerase chain reaction (qRT-PCR) method and SYBR Green (2× qPCRBIO SyGreen Mix Lo-ROX Kit; PCR Biosystems).

qRT-PCR

The cDNAs synthesized from the isolated RNA samples were used to assess gene expression via qRT-PCR according to the Power Sybeer Green qPCR MasterMix protocol (Thermo Fisher Scientific, USA). The expression levels of *BAX* and *p53*, components of the apoptosis pathway, were determined in the control and administration groups of OVCAR3 cells. Actin beta (*ACTB/β-actin*) was used as the reference housekeeping gene. The expression of the selected and housekeeping genes was analyzed using the CFX96 Real-Time PCR Detection System (Bio-Rad). The untreated groups were used as the control. The forward and reverse primer sequences used in the qRT-PCR reactions are listed in Table 1. The qRT-PCR reaction conditions were as follows: incubation at 95°C for 2 minutes; 95°C for 5 seconds, 40 cycles; 66°C for 45 seconds, 45 cycles; 74°C for 2 minutes, 45 cycles; and finally 72°C for 5 minutes, one cycle. The relative mRNA levels were determined using the $2^{-\Delta\Delta Ct}$ method. All cDNA and standard samples were analyzed in triplicate to reduce experimental errors and differences in the same group and under the same conditions. The mRNA levels of the endogenous controls glyceraldehyde 3-phosphate dehydrogenase (*GAPDH*) and *β-actin* were used as calibration and correction factors with the multiple control method.

Western blot

OVCAR3 cells were cultured in 75 cm^2 culture flasks and treated at different times with RA and DOX at their 48-hour IC_{50} values. Next, the medium was removed from the flasks, and the collected cells were mixed with 500 µL of RIPA lysis buffer, 2 µL of phenylmethylsulfonyl fluoride solution, 2 µL of sodium orthovanadate solution, and 2 µL of protease inhibitor (RIPA Lysis Buffer System; Santa Cruz Biotechnology, USA) and homogenized using a Daihan 15D tissue homogenizer under cold conditions at 27,000 rpm. Then, the homogenate was centrifuged at 800 g, and the supernatant was then centrifuged at 14,000 g for 30 minutes. Next, the supernatant was analyzed for the release of mitochondrial proteins. The protein concentration was determined using an Optizen Nano Q spectrophotometer (Mecasys, Korea). Then, the proteins were loaded onto NuPAGE® Bis-Tris polyacrylamide gels (10%) and electrophoresed. Next, the separated proteins were electrotransferred to nitrocellulose membranes. Then, nonspecific sites on the membrane were blocked with a blocking solution overnight at 4°C. Next, the membrane was treated with monoclonal primary antibodies against p53 (Cat. no: MA5-12571, Invitrogen), BAX (Cat. no: MA5-14003, Invitrogen), and β-actin (Cat. no: MA1-140, Invitrogen). Finally, it was incubated with labeled secondary antibodies and observed with the Micro ChemiDoc gel imaging system (DNR Bio-Imaging Systems Ltd., USA). Band densities were determined using GelQuant software.

Wound healing

OVCAR3 cells were seeded in six-well cell culture plates at approximately 200,000 cells/well. When the cells reached sufficient density, a wound was made in the cells adhered to the well floor using a sterile 200 µL volume micropipette tip. After wounding, the disturbed cells were removed from the well by washing with Dulbecco's phosphate-buffered saline (Gibco, USA). Next, serum-free medium containing the vehicle, DOX (72-hour IC_{50}), RA (72-hour IC_{50}), or DOX+RA (72-hour IC_{50}) agents were added to these wells. Then, the cells were imaged using the Thermo EVOS® FL Imaging System at hour 0, and the wound in the control group was monitored until it had completely healed. In the control group, the experiment was terminated after 36 hours, when the wound was 90-100% closed, and the wound healing processes (cell migration) in the treatment groups were imaged.

Statistical analysis

After cell viability rates were determined with the MTT method, the mean mRNA levels obtained by qRT-PCR were compared between groups using one-way analysis of variance (ANOVA) with post-hoc Tukey's honestly significant difference (HSD) tests. Data were compared between two groups using independent samples t-tests, accounting for the homogeneity of the

Table 1. The primers used to quantify the expression of the selected genes.

p53	F: CACGAGCGCTGCTCAGATAGC	R: ACAGGCACAAACACGCACAAA
BAX	F: TTCATCCAGGATCGAGCAGA	R: GCAAAGTAGAAGGCAACG
β-actin	F: CCTCTGAACCCTAAGGCCAAC	R: TGCCACAGGATTCCATACCC
GAPDH	F: CGGAGTCAACGGATTTGGTCGTAT	R: GCCTTCTCCATGGTGGTGAAGAC

All primers are shown in the 5' to 3' direction. F: forward, R: reverse.

data. A $p \leq 0.05$ was considered statistically significant.

Results

Effects of DOX on the viability of OVCAR3 and HaCaT cells

No IC_{50} was found after treating OVCAR3 cells with DOX and RA for 24 hours. As the doses of the applied agents increased, cell proliferation decreased significantly. The initial cell density was 100,000 cells/well, and when treated with 50 mM DOX, the mean number of cells was determined as 103,232 after 24 hours, 23,314 after 48 hours, and 8,686 after 72 hours (Fig. 1). The 48-hour IC_{50} was determined as 2.26 µM DOX for the OVCAR3 cells; after this dose, cell viability was significantly reduced compared to the vehicle (Fig. 1). Similarly, the 48 hour IC_{50} was determined as 6.72 µM DOX for HaCaT cells (Fig. 2).

Effect of RA on the viability of OVCAR3 and HaCaT cells

No IC_{50} was found when treating HaCaT cells with RA for 24, 48, or 72 hours. In addition, no IC_{50} was found when treating OVCAR3 cells with RA for 24 hours. The mean viability of OVCAR3 cells treated with RA was estimated at 70.0% (Fig. 3). The mean survival of HaCaT cells treated with RA was estimated at 76.2% for all treatment durations (Fig. 4). Based on the IC_{50} values, the viability of OVCAR3 cells was significantly reduced. When the effects of treatment with RA and DOX were compared, OVCAR3 cell viability decreased more with DOX.

Effects of RA and DOX on apoptosis in OVCAR3 cells

In order to confirm that the cell death observed in the MTT analysis was via apoptosis, OVCAR3 cells treated with RA and DOX were stained with the NucBlue reagent. The cell death rate was elevated in cells treated with RA and DOX, with the increase dependent on the dose applied. With NucBlue staining, microscopic images showed that apoptosis was not severe in the 48 hour RA group, apoptotic body formation was increased in the 48 hour DOX group, and apoptosis was quite severe with nuclear morphology

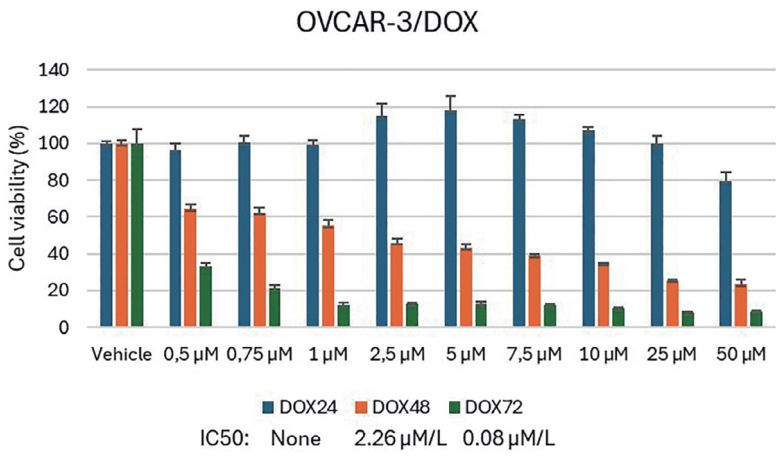

Fig. 1. The effect of nine DOX concentrations (0.5-50 μM) on OVCAR3 cells compared to the vehicle and the IC_{50} for DOX (n=6; the data are presented as the mean ± standard deviation; IC_{50} values were estimated by probit analysis).

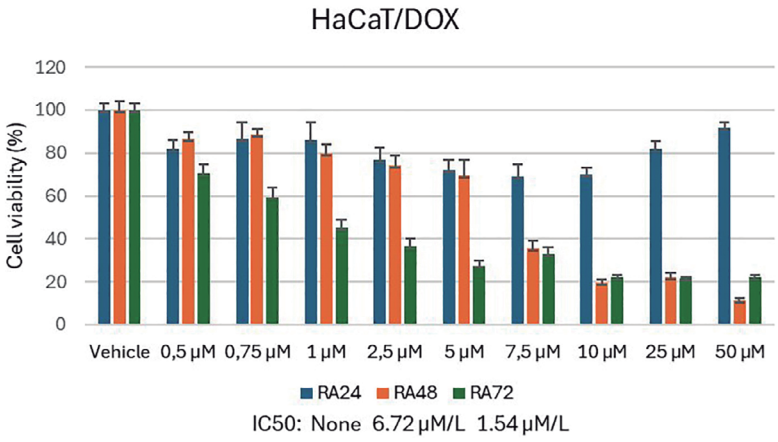

Fig. 2. The effect of nine DOX concentrations (0.5-50 μM) on HaCaT cells compared to the vehicle and the IC_{50} for DOX (n=6; the data are presented as the mean ± standard deviation; IC_{50} values were estimated by probit analysis).

abnormalities in the 48 hour DOX+RA group (Fig. 5).

qRT-PCR and Western blot findings

Based on the NucBlue staining results, the gene expression of proapoptotic *p53* and *BAX* were examined in OVCAR3 cells treated with RA, DOX, and DOX+RA for 48 hours (Fig. 6). All experimental groups comprised nine samples, and the mRNA levels of *p53*, *BAX*, and *β-actin* (endogenous control) were quantified by qRT-PCR. The expression of *p53*, *BAX*, and *β-actin* could be detected, their levels were determined, and amplification curves were created. In the amplification curves, the x-axis represented the number of cycles, and the y-axis represented the normalized reporter (Rn) value.

The increase in *p53* and *BAX* mRNA levels was very small in the control group (Fig. 6A). The increase in *p53* mRNA levels was significantly greater in the DOX and RA groups than in the control group. However, the increase in *p53* mRNA levels did not differ significantly between the DOX group and the DOX+RA and RA groups.

While *BAX* mRNA levels differed significantly between the control group and the DOX (p=0.003), RA (p=0.003), and DOX+RA (p=0.006) groups, as well as between the RA group and the DOX+RA group (p=0.005; Fig. 6B). However, *BAX* mRNA levels did not differ significantly between the control and DOX+RA groups and between the DOX and RA groups.

In contrast, *BAX* mRNA levels increased significantly after 12 hours and differed significantly between the control group and the RA and DOX groups after 48 hours ($p \leq 0.003$; Fig. 6B). The Western blot analysis also showed that DOX and RA increased the protein levels of BAX and p53 (Fig. 7).

Effect of RA and DOX on wound healing

Cell motility was assessed by wound healing analysis. Treatment with RA, DOX, and DOX+RA significantly decreased the wound healing ability of OVCAR3 cells after 36 hours compared to the control (p<0.01; Fig. 8). It was determined that treatment with DOX and RA individually caused proximal cell

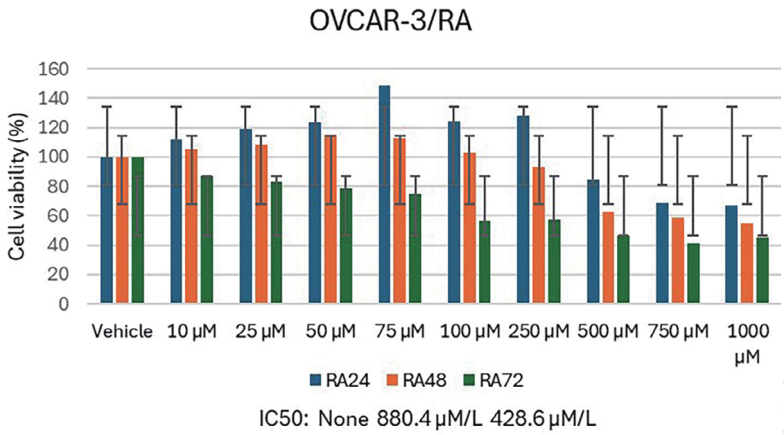

Fig. 3. The effect of nine RA concentrations (10-1000 μM) on OVCAR3 cells after 24, 48, and 72 hours (n=6; the data are presented as the mean ± standard deviation; IC_{50} values were estimated by probit analysis).

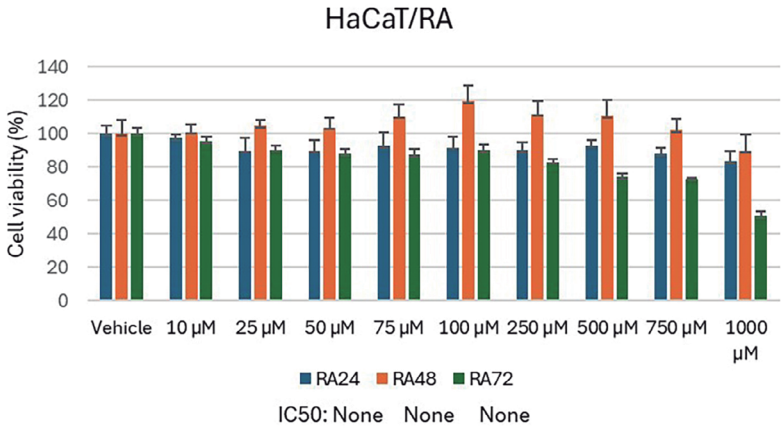

Fig. 4. The effect of nine RA concentrations (10-1000 μM) on HaCaT cells after 24, 48, and 72 hours (n=6; the data are presented as the mean ± standard deviation; IC_{50} values were estimated by probit analysis).

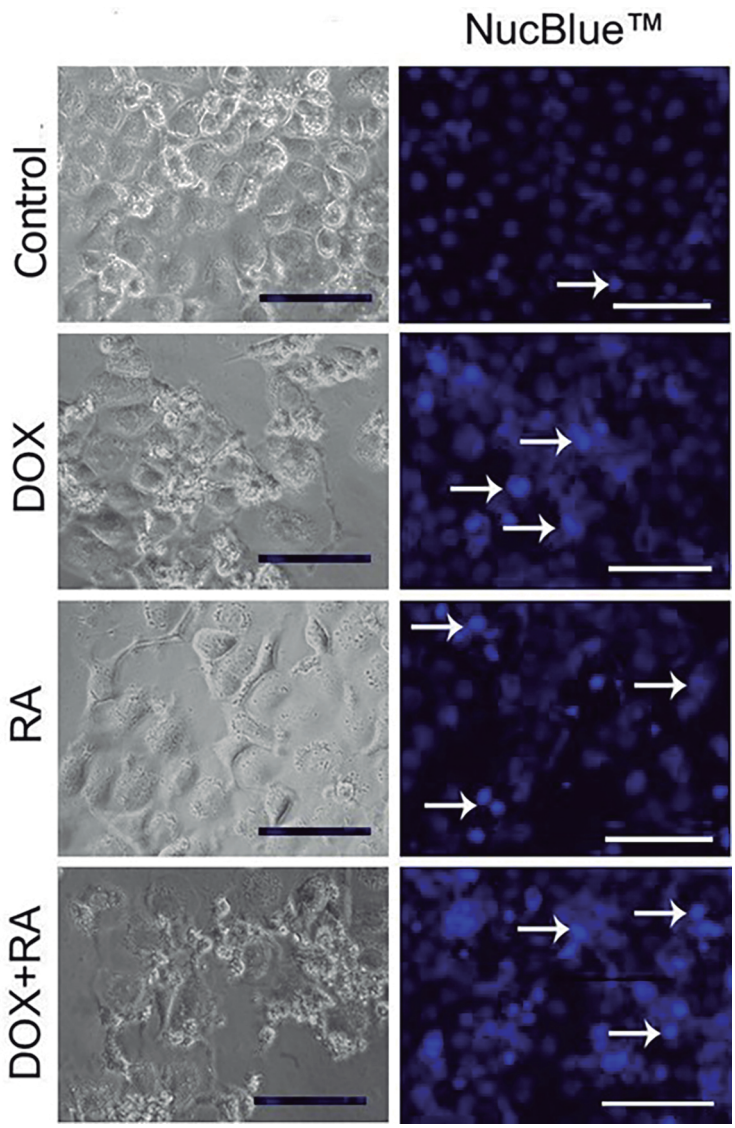

Fig. 5. Cell morphology and apoptotic body formation in OVCAR3 cells treated with RA, DOX, and DOX+RA (arrow: apoptotic cell). Scale bars: 50 µm.

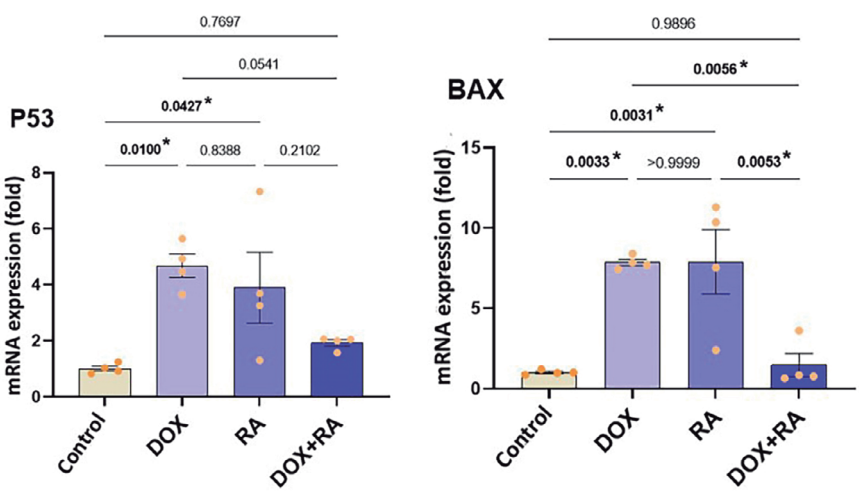

Fig. 6. Relative fold increases in p53 and BAX mRNA levels in OVCAR3 cells treated with DOX (IC_{50}) and RA (IC_{50}) for 48 hours alone and in combination (the control represents a multiple control with *β-actin* and *GAPDH* mRNA levels; n=4; the data are presented as the mean ± standard deviation). * denotes means that differed significantly in one-way ANOVA with post-hoc Tukey's HSD tests.

migration (Fig. 8).

Discussion

Our study investigated the antiproliferative effects of RA on an ovarian carcinoma cell line, focusing on its role in modulating the p53/BAX signaling pathway. Our findings demonstrate that RA significantly inhibits proliferation and induces apoptosis in ovarian cancer cells. Activation of the p53/BAX pathway appears to be a key mechanism underlying these effects. Our results align with previous studies highlighting the anticancer potential of RA and provide new insights into its molecular actions. This discussion will explore the implications of our findings in the context of existing literature, address the potential limitations of our study, and suggest future research directions to further elucidate the therapeutic potential of RA in ovarian cancer treatment.

The incidence of ovarian cancer is seriously increasing among women, and many studies have shown that it ranks first among cancers. Paclitaxel with carboplatin is used as a first-line chemotherapy regimen in patients with ovarian cancer. However, two large randomized controlled trials comparing carboplatin with

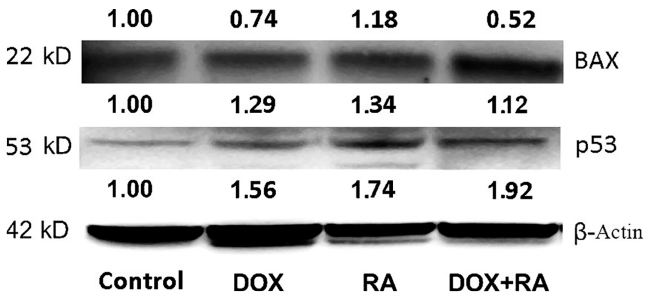

Fig. 7. Western blot of BAX and p53 protein levels. RA and DOX treatment increased p53 and BAX protein levels.

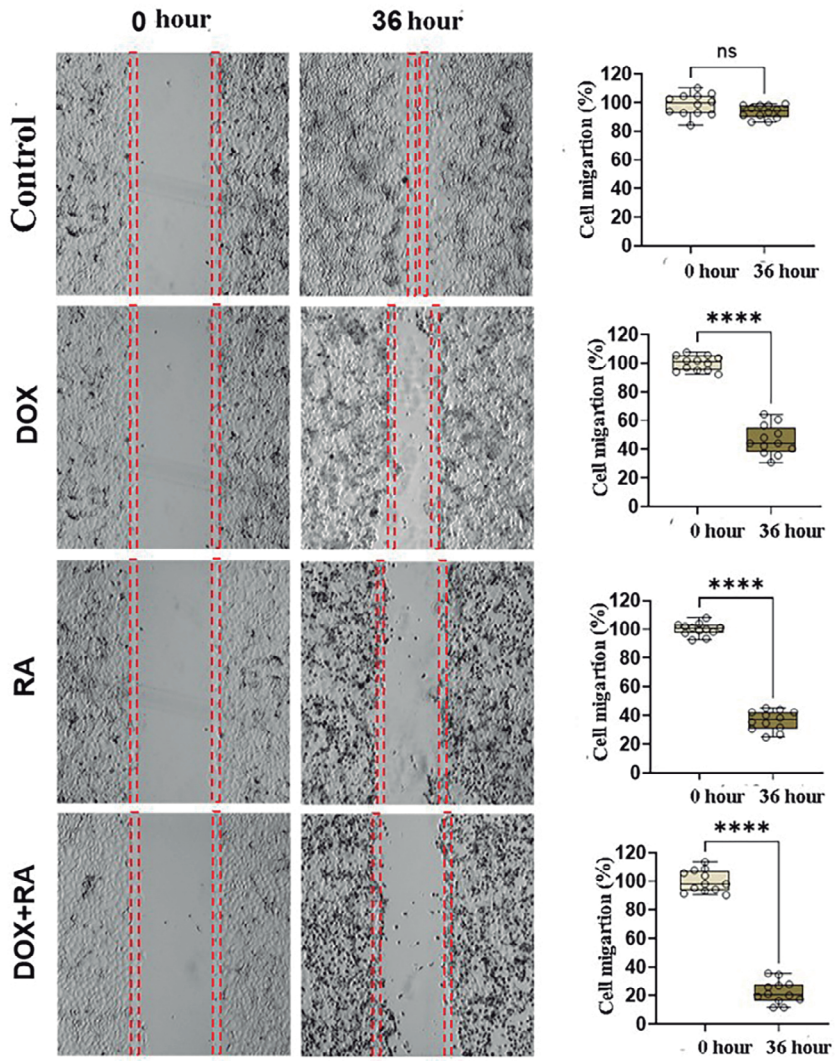

Fig. 8. Cell migration rate and percentage wound closure determined by wound healing assay (after 36 hours) in OVCAR3 cells treated with vehicle (control), DOX, RA, and DOX+RA at their IC_{50} (n=12; bars represent the mean ± standard error; * significantly different [$p \leq 0.001$] based on an independent samples t-test).

pegylated liposomal DOX to carboplatin with paclitaxel showed that carboplatin with DOX is as effective as standard therapy with carboplatin and paclitaxel. Pegylated liposomal DOX is also a treatment option for relapsed or platinum-resistant ovarian cancer, but there is no clear distinction between monotherapy options in this setting. Our results suggest that pegylated liposomal DOX is as effective as other monotherapies and more tolerable. Therefore, they reported that it might be the preferred agent in the palliative setting (Li et al., 2021). An *in vitro* study found that combination treatment with DOX and thymoquinone decreased the proliferation of an ovarian cancer cell line (Karaosmanoğlu et al., 2024).

Studies suggest that RA plays an important role in preventing cancer, reducing the effects of chemotherapy drugs used in its treatment, and ensuring the death of cancer cells. Our study aimed to demonstrate the biological effects of RA on OVCAR3, a cell line resistant to ovarian cancer. To achieve this goal, we evaluated and revealed the effects of RA on p53/BAX, one of the most researched intracellular signaling pathways. One study reported that RA increases the BAX/BCL2 apoptosis regulator (BCL2) ratio, proteins belonging to the active caspase family that inhibit poly(ADP-ribose) polymerase (PARP), causing apoptosis in several tumor cell lines (Jin et al., 2020). Another study has shown that RA supports the activity of the caspase family in different tumor cells *in vitro*, including lung cancer, oral cancer, glioma, and osteosarcoma (Ma et al., 2020).

Many studies have shown that RA is preventive in chemotherapy by inhibiting the nuclear factor kappa B (NF-κB)/p53/caspase 3 (CASP3) pathway. An *in vivo* study has shown that the levels of apoptotic markers caspase, p53, and BCL2 decreased when mice were treated with 100 mg/kg RA one week before in an experimental cancer model (Moore et al., 2016). In addition, RA appears to be used in many cancer treatments due to its many properties, including apoptosis, metastasis, and inflammation, preventing the proliferation of tumor cells in cancer. Ma et al. (2020) revealed that RA causes apoptosis in cancer cells by suppressing the BCL2/BAX ratio and increasing caspase cleavage through mitochondrial apoptotic pathways. Another study has shown that BCL2 and BAX gene and protein expression decreases after breast cancer treatment with RA. A similar study revealed that RA inhibited tumor growth through mitochondrial apoptotic pathways and caspase cleavage. Moreover, NF-κB has been implicated in many cancer pathways, including inflammation, angiogenesis, and apoptosis, and has been shown to play an important role in cancer prognosis and drug resistance (Li et al., 2019). It was observed that applying RA alone was not very effective on apoptosis. However, administering RA together with chemotherapy agents was very effective in causing apoptosis. Unlike in other studies, when we examined the antiapoptotic effects of RA on the OVCAR3 cell line, we found that RA alone could be an important initiator of apoptosis and exhibited similar proapoptotic activity to DOX. However, administering RA with DOX decreased the expression of p53 and BAX, suggesting that RA plays an inhibitory and antiapoptotic role in OVCAR3 cells through the proapoptotic pathway. Therefore, it may be important to choose new therapeutics along with drugs used to suppress cell proliferation instead of increasing the dose during chemotherapy. Increased nuclear fragmentation was also detected, indicative of the occurrence of apoptosis.

Another study predicted that using cisatracurium could increase the expression of p53 and long noncoding RNA (lincRNA)-p21 in OVCAR3 ovarian cancer cells in a dose-dependent manner. Compared to the control group, lincRNA-p21 knockdown inhibited the proliferation, migration, and invasion of OVCAR3 cells and induced apoptosis. These results revealed that lincRNA-p21 can be used as a treatment for ovarian cancer due to its tumor suppression (Zhu et al., 2021). Another study evaluated human ovarian cancer lines OVCAR3 and A2780/CP70 treated with gallic acid (GA) for 24, 48, and 72 hours, revealing that GA exposure had higher IC_{50} values. It was also determined that GA had stronger suppressive effects on OVCAR3 cells than on A2780/CP70 cells. In addition, the IC_{50} for GA decreased in both cell lines when the treatment duration increased from 24 to 72 hours (He et al., 2021).

Interleukin (IL)-8 is an inflammatory factor and a very important biomarker of disease prognosis. Studies have shown that RA inhibits the bone metastasis of breast cancer cells by inhibiting the expression of IL-8 via the NF-κB pathway. Although the exact interaction of this interaction is unclear, it has been revealed that RA has an antimetastatic effect and antioxidant properties. Other studies have revealed that RA inhibits NF-κB signaling by stimulating antioxidant enzymes through reactive oxygen species scavenging or suppression (Konstantinou et al., 2023). Therefore, RA is used as an antitumor agent and multidrug resistance (MDR) reversal agent in different cancers. The antitumor effect of RA and whether it can reverse MDR in non-small cell lung cancer (NSCLC) are largely unknown. One of the anti-MDR mechanisms is inhibiting P-glycoprotein (P-gp) expression and function. Accordingly, one study examined the potential antitumor and drug resistance reversal activity of RA, revealing that RA did not affect the proliferation of normal cells up to a concentration of 14.05 μg/mL, with an IC_{50} of 29.52 μg/mL (Liao et al., 2020). Another study examined the BCL2/BAX signaling pathway and highlighted that RA combined with cisplatin could significantly reduce BCL2 expression in A549 and A549DDP cells. It has been demonstrated that RA can reverse MDR in NSCLC by modulating complex signaling (Zhao et al., 2022). The methods used in these studies have shown that anticancer agents do not have cytotoxicity independent of chemotherapy. Therefore, new methods are being explored to elucidate the mechanisms of action and identify new molecules with

the most powerful anticancer properties and the fewest side effects.

In conclusion, our study provides compelling evidence that RA exerts significant antiproliferative and proapoptotic effects on ovarian carcinoma cell lines. The activation of the p53/Bax signaling pathway appears to be a critical mechanism mediating the anticancer effects of RA. Our findings not only enhance our understanding of the molecular actions of RA but also underscore its potential as a promising therapeutic agent for treating ovarian cancer. However, further *in vivo* studies and clinical trials are needed to validate our results and explore the safety and efficacy of RA in patients with cancer. Overall, our study contributes to the growing body of evidence supporting the use of natural compounds in cancer therapy and highlights the need for continued investigation into their mechanisms of action.

References

Achour M., Bravo L., Sarriá B., Ben Fredj M., Nouira M., Mtiraoui A., Saguem S. and Mateos R. (2021). Bioavailability and nutrikinetics of rosemary tea phenolic compounds in humans. Food Res. Int. 139, 109815.

Chandra A., Pius C., Nabeel M., Nair M., Vishwanatha J.K., Ahmad S. and Basha R. (2019). Ovarian cancer: Current status and strategies for improving therapeutic outcomes. Cancer Med. 8, 7018-7031.

Emery J., Butow P., Lai-Kwon J., Nekhlyudov L., Rynderman M. and Jefford M. (2022). Management of common clinical problems experienced by survivors of cancer. Lancet 399, 1537-1550.

Ganesan K., Du B. and Chen J. (2022). Effects and mechanisms of dietary bioactive compounds on breast cancer prevention. Pharmacol. Res. 178, 105974.

He Z., Liu X., Wu F., Wu S., Rankin G.O., Martinez I., Rojanasakul Y. and Chen Y.C. (2021). Gallic acid induces S and G2 phase arrest and apoptosis in human ovarian cancer cells *in vitro*. Appl. Sci. 11, 3807.

Homayoun M., Seghatoleslam M., Pourzaki M., Shafieian R., Hosseini M. and Bideskan A.E. (2015). Anticonvulsant and neuroprotective effects of Rosa damascena hydro-alcoholic extract on rat hippocampus. Avicenna J. Phytomed. 5, 260-270.

Jin B., Liu J., Gao D., Xu Y., He L., Zang Y., Li N. and Lin D. (2020). Detailed studies on the anticancer action of rosmarinic acid in human Hep-G2 liver carcinoma cells: evaluating its effects on cellular apoptosis, caspase activation and suppression of cell migration and invasion. J. BUON 25, 1383-1389.

Jin B.R., Chung K.S., Hwang S., Hwang S.N., Rhee K.J., Lee M. and An H.J. (2021). Rosmarinic acid represses colitis-associated colon cancer: A pivotal involvement of the TLR4-mediated NF-κB-STAT3 axis. Neoplasia 23, 561-573.

Karaosmanoğlu Ö., Kamalak Z., Özdemir İ., Öztürk Ş. and Tuncer M.C. (2024). Apoptotic effect of thymoquinone on OVCAR3 cells via the P53 and CASP3 activation. Acta Cir. Bras. 39, e399224.

Konstantinou E.K., Panagiotopoulos A.A., Argyri K., Panoutsopoulos G. I., Dimitriou M. and Gioxari A. (2023). Molecular pathways of rosmarinic acid anticancer activity in triple-negative breast cancer cells: A literature review. Nutrients 16, 2.

Li W., Li Q., Wei L., Pan X., Huang D., Gan J. and Tang S. (2019). Rosmarinic acid analogue-11 induces apoptosis of human gastric cancer SGC-7901 cells via the Epidermal Growth Factor Receptor (EGFR)/Akt/Nuclear Factor kappa B (NF-κB) pathway. Med. Sci. Monit. Basic Res. 25, 63-75.

Li X.R., Zhu Y., Zhang G.N., Huang J.M. and Pei L.X. (2021). The impact of Pegylated liposomal doxorubicin in recurrent ovarian cancer: an updated meta-analysis of randomized clinical trials. J. Ovarian Res. 14, 42.

Liao X.Z., Gao Y., Sun L.L., Liu J.H., Chen H.R., Yu L., Chen Z.Z., Chen W.H. and Lin L.Z. (2020). Rosmarinic acid reverses non-small cell lung cancer cisplatin resistance by activating the MAPK signaling pathway. Phytother. Res. 34, 1142-1153.

Ma Z., Yang J., Yang Y., Wang X., Chen G., Shi A., Lu Y., Jia S., Kang X. and Lu L. (2020). Rosmarinic acid exerts an anticancer effect on osteosarcoma cells by inhibiting DJ-1 via regulation of the PTEN-PI3K-Akt signaling pathway. Phytomedicine 68, 153186.

Magalhães D.B., Castro I., Lopes-Rodrigues V., Pereira J.M., Barros L., Ferreira, I.C.F.R., Xavier C.P.R. and Vasconcelos M.H. (2018). Melissa officinalis L. ethanolic extract inhibits the growth of a lung cancer cell line by interfering with the cell cycle and inducing apoptosis. Food Funct. 9, 3134-3142.

Moore J., Yousef M. and Tsiani E. (2016). Anticancer effects of rosemary (*Rosmarinus officinalis* L.) extract and rosemary extract polyphenols. Nutrients 8, 731.

Pokhriyal R., Hariprasad R., Kumar L. and Hariprasad G. (2019). Chemotherapy resistance in advanced ovarian cancer patients. Biomark. Cancer 11, 1179299X19860815.

Siegel R.L., Miller K.D., Fuchs H.E. and Jemal A. (2022). Cancer statistics, 2022. CA Cancer J. Clin. 72, 7-33.

Torre L.A., Trabert B., DeSantis C.E., Miller K.D., Samimi G., Runowicz C.D., Gaudet M.M., Jemal A. and Siegel R.L. (2018). Ovarian cancer statistics, 2018. CA Cancer J. Clin. 68, 284-296.

Zhao J., Xu L., Jin D., Xin Y., Tian L., Wang T., Zhao D., Wang Z. and Wang J. (2022). Rosmarinic acid and related dietary supplements: Potential applications in the prevention and treatment of cancer. Biomolecules 12, 1410.

Zhu D., Shi C., Jiang Y., Zhu K., Wang X. and Feng W. (2021). Cisatracurium inhibits the growth and induces apoptosis of ovarian cancer cells by promoting lincRNA-p21. Bioengineered 12, 1505-1516.

Accepted February 5, 2025